

Excitation Function for the $Mg^{25}(p, 2p)Na^{24}$ Reaction in the GeV Energy Region*

PAUL L. REEDER

Chemistry Department, Washington University, Saint Louis, Missouri 63130 and

Chemistry Department, Brookhaven National Laboratory, Upton, New York 11973

(Received 3 September 1968)

The cross section for the $Mg^{25}(p, 2p)Na^{24}$ reaction was measured at 8 energies from 0.43 GeV to 2.7 GeV. The cross sections increased from 26.7 ± 0.8 mb at 0.43 GeV to 31.9 ± 1.0 mb at 1.01 GeV. As expected from the clean-knockout mechanism, this increase is related to a large increase in free-particle cross section. An empirical expression which takes into account the momentum of the struck particle and a rough estimate of attenuation factors gives a reasonable fit to all cross-section data from 0.15 to 2.7 GeV. Monte Carlo calculations at 0.15 GeV also agree with the experimental cross sections. Effective forward and backward ranges for Na^{24} in Mg^{25} were measured, using the thick-target-thick-catcher technique.

INTRODUCTION

AT GeV energies, simple nuclear reactions such as the (p, pn) and $(p, 2p)$ reactions are assumed to proceed by a clean-knockout mechanism.¹ This mechanism consists of a single "quasifree" collision between the incident nucleon and a nucleon of the target. Both collision partners and any mesons created by the collision escape without exciting the nucleus to the point of emitting additional nucleons. The nucleon-nucleon collision is considered to be "quasifree" since effects due to the momentum distribution of the struck nucleon and to the Pauli exclusion principle must be accounted for. The free-particle cross sections must be corrected for these effects to obtain the effective cross sections for collisions within nuclear matter.²

Prominent structure in the free-particle cross sections influences the cross sections for simple nuclear reactions as previously observed in the excitation functions for the $C^{12}(\pi^-, \pi^-n)C^{11}$ reaction^{3,4,5} and the $Ar^{40}(\pi^-, \pi^-p)Cl^{39}$ reaction.⁶ In these reactions, pronounced structure was observed which correlated with resonances in the π^-n and π^-p free-particle cross sections. However, the pn free-particle cross section does not have significant structure. The measured cross sections for the (p, pn) reactions are thus rather smooth functions of bombarding energy and generally decrease gradually from 0.3 to 3.0 GeV.⁷ The pp free-particle cross section rises by a factor of 2 from 0.4 to 1.0 GeV, but relatively few $(p, 2p)$ excitation functions have been measured in this energy region. The $Ce^{142}(p, 2p)La^{141}$ reaction has been the subject of

several investigations.^{8,9,10} The most recent of these¹⁰ has shown that this excitation function rises by a factor of 1.47 ± 0.13 in going from 0.42 to 1.0 GeV and decreases slowly above 1.0 GeV. The $Zn^{68}(p, 2p)Cu^{67}$ and $Fe^{57}(p, 2p)Mn^{56}$ reactions also indicate a rise in cross section from 0.4 to 0.72 GeV and a constant energy dependence from 2.2 to 6.2 GeV.¹¹

More accurate measurements of the $(p, 2p)$ excitation functions are desirable. If a suitable method of treating the attenuation factors of the incident and outgoing particles were used, it would be possible to calculate a momentum distribution for the struck nucleon based on the smearing out of the rise in pp free-particle cross sections.

The accuracy of the radiochemical techniques used to measure the $(p, 2p)$ excitation functions mentioned above is limited by errors in determining the chemical yields and in determining the absolute counting efficiency for the product and monitor radioactivities. The present experiment eliminates these two sources of error and provides a measurement on a light mass nuclide where the large surface-to-volume ratio might enhance the effect of the free-particle cross sections.

EXPERIMENTAL

The monitor reaction most commonly used for high-energy radiochemical measurements is $Al^{27}(p, 3pn)Na^{24}$.¹² The $Mg^{25}(p, 2p)Na^{24}$ reaction thus gives the same product as the monitor reaction. In both cases, the β activity from Na^{24} can easily be distinguished from any other radioactivity produced in the bombardment without resorting to chemical separations. This eliminates the problem of determining a chemical yield and its associated uncertainty. The β counting efficiency for Na^{24} in the magnesium target is the same as that of Na^{24} in the aluminum monitor foil except

⁸ A. A. Caretto and G. Friedlander, *Phys. Rev.* **110**, 1169 (1958).

⁹ B. M. Foreman, Jr., *Phys. Rev.* **132**, 1768 (1963).

¹⁰ S. Meloni and J. B. Cumming, *Phys. Rev.* **136**, B1359 (1964).

¹¹ P. L. Reeder, University of California Radiation Laboratory Report No. UCRL-10531, 1962 (unpublished).

¹² J. B. Cumming, *Ann. Rev. Nucl. Sci.* **13**, 261 (1963).

* Research performed at Brookhaven National Laboratory under the auspices of the U.S. Atomic Energy Commission.

¹ J. R. Grover and A. A. Caretto, *Ann. Rev. Nucl. Sci.* **14**, 51 (1964).

² T. Clements and L. Winsberg, *Phys. Rev.* **122**, 1623 (1961).

³ P. L. Reeder and S. S. Markowitz, *Phys. Rev.* **133**, B639 (1964).

⁴ A. M. Poskanzer and L. P. Remsburg, *Phys. Rev.* **134**, B779 (1964).

⁵ S. Kaufman and C. O. Hower, *Phys. Rev.* **154**, 924 (1967).

⁶ C. O. Hower and S. Kaufman, *Phys. Rev.* **144**, 917 (1966).

⁷ S. S. Markowitz, F. Rowland, and G. Friedlander, *Phys. Rev.* **112**, 1295 (1958).

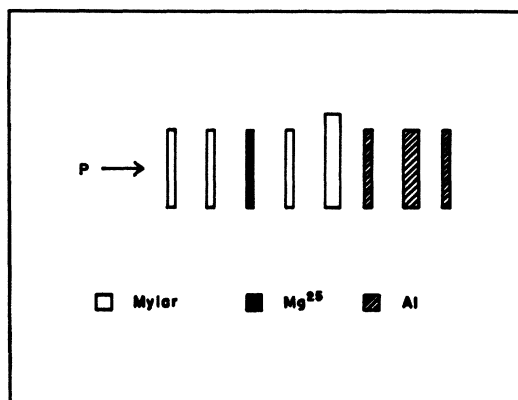


FIG. 1. Target stack.

for a small correction for differences in foil thicknesses. This procedure minimizes the uncertainty in efficiency factors for the monitor and product activities.

The Mg^{25} target material (enriched to 99.49% Mg^{25}) was supplied as a 1-in.-square foil¹³ which was then cut into four 0.5-in. squares. The surface density of each foil was determined by weight and area measurements and varied from 7.16 to 10.48 mg/cm². The Mg^{25} foil was sandwiched between two 0.001-in.-thick Mylar foils which served to catch any Na^{24} which recoiled either forwards or backwards. These three foils were counted individually and the Na^{24} activity from all three was combined to give the total Na^{24} activity from Mg^{25} . In addition, the fractions of the Na^{24} activity which recoiled forward or backwards were determined to obtain the forward and backward ranges.

The monitor foil was a piece of 0.003-in. aluminum foil. This was sandwiched between two pieces of 0.001-in. aluminum foil. In this case, the Na^{24} recoiling forward or backward from the monitor foil was assumed to be compensated for by recoil in from the guard foils. Only the Na^{24} activity in the 0.003-in. foil was used for the monitor activity.

The target stack was separated from the monitor stack by a piece of 0.003-in. Mylar which extended 3 mm beyond the leading edges of the other foils. This served to scatter the incident beam and gave a more uniform distribution of activity.

An additional 0.001-in. Mylar foil was placed before the target stack to protect the upstream catcher foil from Na^{24} produced in other parts of the accelerator. This foil was counted in the same manner as the Mylar catcher foils and the data were used to estimate the activation blank correction.

The complete target stack is illustrated in Fig. 1. The total thickness of the target stack was about 65 mg/cm². Except for the Mg^{25} foil and the foil with the lip, the foils were punched from a 0.5-in. square press. The leading edges were carefully aligned by eye before placing the stack in the target holder. The

leading edge was never trimmed or machined as is sometimes done since the Mg^{25} foils were re-used for several bombardments.

The distribution of activity as a function of distance from the leading edge was checked at two bombarding energies, 0.4 and 2.0 GeV. The upstream Al guard foil was cut into 2.5-mm strips. The β activity of these strips when plotted as a function of distance from the leading edge gave an exponential curve with a half-distance of 3 mm at both energies. A single 0.003-in. aluminum foil used as a dummy target at 2.0 GeV gave the same distribution. An additional check on a downstream aluminum guard foil at 0.8 GeV showed that the ratio of F^{18} activity to Na^{24} activity was constant as a function of distance from the leading edge. These tests indicate that with the bombarding conditions used here the product distribution is not very sensitive to beam energy, target thickness, or complexity of the reaction. It is estimated that the leading edges of the target stack were aligned to within 0.25 mm, which would correspond to an uncertainty of less than 5% in the ratio of product activity to monitor activity. The alignment of the leading edges is thought to be the largest source of error, as will be discussed later.

The vertical distribution of the beam was observed in a radioautograph of a dummy target and showed that the beam height was smaller than the 0.5-in. targets.

The targets were bombarded in the internal beam of the Cosmotron for about 10 min. Targets were mounted on a breech loading ram in the south straight section. A thick shutter target was mounted on a ram in the east straight section to shield the target from low-energy protons during the early stages of the acceleration cycle. In normal operation the target was stationary while the shutter was withdrawn just before the end of the acceleration cycle and replaced before the injection of the next beam pulse. Each series of experiments consisted of four bombardments—two targets each at two energies. Four series were performed

TABLE I. Cross sections for the $Mg^{25}(p, 2p)Na^{24}$ reactions.

Beam energy (GeV)	Cross section (mb)	Monitor cross section (mb)
0.43±0.01	26.7±0.8	10.6
0.63±0.01	29.8±0.9	10.8
0.81±0.01	30.7±0.9	10.8
1.01±0.01	31.9±1.0	10.5
1.18±0.02	29.1±3.0	10.25
1.52±0.02	28.5±0.9	9.8
2.00±0.02	24.8±0.8	9.5
2.70±0.05	26.3±0.8	9.2

¹³ Supplied by Oak Ridge National Laboratory.

TABLE II. Recoil data for Mg²⁵(p, 2p)Na²⁴ reaction.

Beam energy (GeV)	Forward/backward ratio	Effective forward range (μg/cm ²)	Effective forward range (MeV)	Effective backward range (μg/cm ²)	Effective backward range (MeV)
0.43±0.01	4.5±0.3	123±6	0.29	27±1	0.060
0.63±0.01	4.3±0.3	125±6	0.30	29±1	0.066
0.81±0.01	4.1±0.3	118±5	0.28	29±1	0.063
1.01±0.01	3.0±0.2	101±6	0.24	34±2	0.076
1.18±0.02	3.0±0.4	106±8	0.25	35±2	0.079
1.52±0.02	2.8±0.2	94±4	0.22	34±2	0.077
2.00±0.02	2.5±0.2	107±5	0.25	43±2	0.100
2.70±0.05	2.6±0.2	102±5	0.24	40±4	0.091

at approximately one week intervals, thus giving two bombardments each at eight energies ranging from 0.43 to 2.70 GeV.

The radius of the equilibrium orbit was measured at each energy and was used with either the magnetic field or rf frequency to calculate the beam energy. The energy uncertainty in Table I is due to a ±1-in. spread in the radius.

After waiting at least 17 h to allow F¹⁸ activity to die out, the foils were mounted on aluminum counting cards and covered with 0.00025-in. Mylar. β counting was performed on end-window gas-flow proportional counters. The aluminum and magnesium foils were counted on a low shelf, whereas the catcher and activation blank foils were counted on a high shelf. The ratio of activities on these shelves was measured with an accuracy of 3%. The total activity in the catcher foils was 2% or less of the total Na²⁴ activity from Mg²⁵.

The decay data were processed by a least-squares decay curve fitting program (CLSQ).¹⁴ This program fit a single component of known half-life (15.0 h) to the data and gave the initial activity of the Na²⁴ at the end of bombardment.

For one series of experiments the Na²⁴ γ rays were counted in a 3-in. by 3-in. NaI detector in addition to the usual β counting. The ratio of Na²⁴ activity in magnesium to Na²⁴ activity in aluminum differed by 5.3±0.5% between the β and γ counting. This effect is attributed to the difference in selfabsorption for β counting between the aluminum (21 mg/cm²) and magnesium (7.2–10.5 mg/cm²) foils. This ratio was constant within experimental error for the four thicknesses of magnesium used. All ratios of Na²⁴ in Mg to Na²⁴ in Al determined by β counting were multiplied by the same factor 1.053±0.005.

CROSS-SECTION RESULTS

The Mg²⁵(p, 2p)Na²⁴ cross sections were calculated from the ratio of initial activities of Na²⁴ for the target and monitor foils, the ratio of the surface densities in atoms per cm² for the monitor and target foils, and the cross section for the monitor reaction.

The monitor cross sections are taken from a review article by Cumming and are assumed to be accurate to about 6%.¹² This uncertainty is not included in the error estimates given below. The cross-section results are presented in Table I. For all energies the average deviation of duplicate measurements was 2.9%. If the data at 1.18 GeV are neglected, the average deviation becomes 1.9%. The expected uncertainties for all factors other than the alignment of the leading edges are all less than 1%. Hence it was assumed that the average deviation of the duplicate measurements was a measure of the alignment of the leading edge. The uncertainties shown in Table I are ±3% except for the cross section at 1.18 GeV, where the deviation from the average value was ±10%.

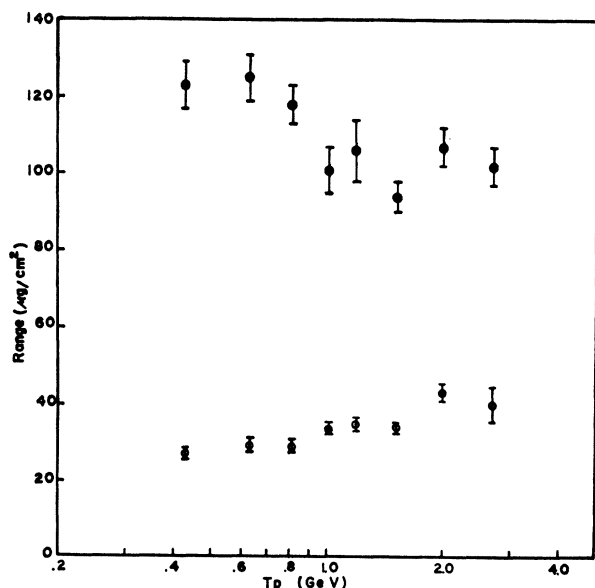


FIG. 2. Effective ranges of Na²⁴ in Mg²⁵ from Mg²⁵(p, 2p)Na²⁴ reaction. Open circles—backward range (BW). Closed circles—forward range (FW).

¹⁴ J. B. Cumming, U.S. Atomic Energy Commission Report No. NAS-NS3107, 1962, p. 25 (unpublished).

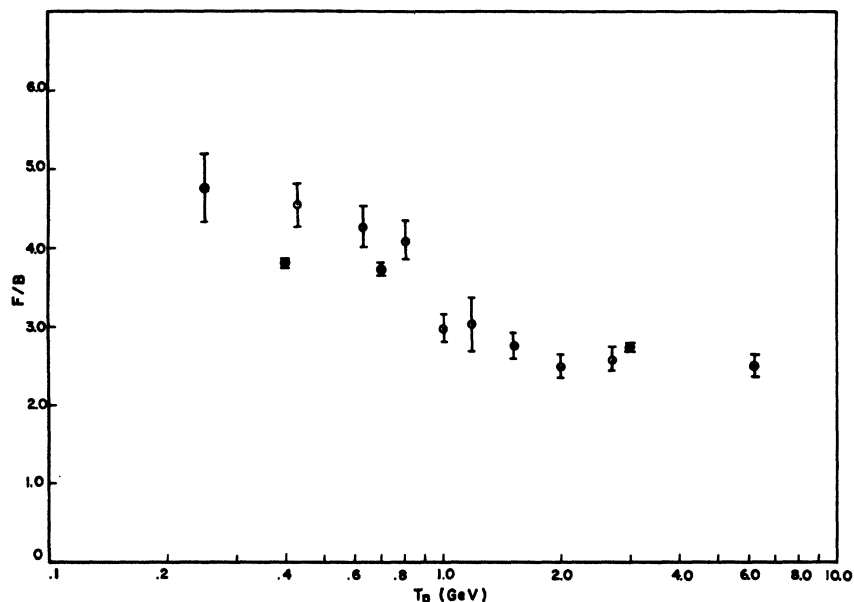


FIG. 3. Forward-backward ratio (F/B). Open circles: Na²⁴ in Mg²⁵ from Mg²⁵($p, 2p$)Na²⁴ reaction. Closed circles: C¹¹ in plastic from C¹²(p, pn)C¹¹ reaction (Ref. 16).

RECOIL-RANGE RESULTS

The effective ranges in the forward and backward directions were measured by means of the thick-target-thick-catcher technique.¹⁵ The effective forward range is defined as FW , where F is the fraction of the total activity which recoils in the direction of the beam and W is the target thickness. Likewise, the effective backward range is BW , where B is the fraction of the total activity observed in the backward direction. The forward-backward ratio ($FW/BW = F/B$) is a convenient measure of the asymmetry of the angular distribution.

The experimental values of FW , BW , and F/B are presented in Table II and are plotted in Fig. 2 and Fig. 3. In Fig. 3 the F/B ratios for the Mg²⁵($p, 2p$)Na²⁴ reaction are compared with the F/B ratios determined for the C¹²(p, pn)C¹¹ reaction.¹⁶

The present data have been corrected for the activation blank determined from the activity in the first foil of each target stack. The largest correction was 12% and the average correction was 4.8%. These data have not been corrected for scattering or edge effects. Scattering effects of about 5% have been measured for recoil ranges of fission fragments in Al.¹⁷ However, the effect is expected to be small when the target and catcher are similar in charge. An edge effect of about 0.5% was observed for recoil ranges of fission fragments from 450-MeV protons on 1-mil U.¹⁷ A direct comparison with this work is not feasible since in the present work the target and catcher foils were the same size. The alignment of the leading edge of the

target and catcher foils is critical for this arrangement and is thought to be the most important contributor to the random error. As with the cross-section measurements, the agreement of duplicate results is taken as the measure of the random error and is shown in Table II as the uncertainty. The average deviation of duplicate measurements is 3.8% for the effective forward range and 3.2% for the effective backward range.

In order to convert the effective ranges to effective energy, a range-energy curve for Na²⁴ ions in Mg²⁵ is needed. Data are available in the literature for Na²⁴ in Al for the energy region from 0.001 to 0.1 MeV¹⁸ and from 1.0 to 2.8 MeV.¹⁹ Experimental errors were about 10 and 5%, respectively. The predicted range-energy curve for Na²⁴ in Al based on the Lindhard-Scharf-Schiott theory²⁰ gives energies which are about 15% lower than the experimental data. The predicted range-energy curve for Na²⁴ in Mg²⁵ gives energies which are about 5% higher than the predictions for Na²⁴ in Al. Therefore, a range-energy curve for Na²⁴ in Mg²⁵ was constructed through the experimental data for Na²⁴ in Al²⁷ and by using the shape of the calculated curves to interpolate between the two sets of experimental data. The effective recoil energies listed in Table II have a systematic uncertainty of about 10% due to the range-energy conversion in addition to the random errors.

DISCUSSION

The excitation function for the Mg²⁵($p, 2p$)Na²⁴ reaction is plotted in Fig. 4. Data for the energy region

¹⁸ M. McCargo, F. Brown, and J. A. Davies, Can. J. Chem. **41**, 2309 (1963).

¹⁹ A. M. Poskanzer, Phys. Rev. **129**, 385 (1963).

²⁰ J. Lindhard, M. Scharff, and H. E. Schiott, Kgl. Danske Videnskab. Selskab, Mat.-Fys. Medd. **33**, No. 14 (1963).

¹⁵ J. M. Alexander, in *Nuclear Chemistry*, edited by L. Yaffe (Academic Press Inc., New York, 1968), Vol. 1.

¹⁶ S. Singh and J. M. Alexander, Phys. Rev. **128**, 711 (1962).

¹⁷ J. A. Panontin and N. Sugarman, J. Inorg. Nucl. Chem. **25**, 1321 (1963).

from 0.125 to 0.404 GeV are from a thesis by Kiely.²¹ The data from 0.08 to 0.11 GeV are by Meadows and Holt.²² Included in the figure are three points for the O¹⁸(p, 2p)N¹⁷ reaction.^{23,24} The solid curve gives the total cross section for pp scattering taken from the compilation by Baraschenkov and Maltsev²⁵ for energies below 1.0 GeV and from Bugg *et al.* for energies above 1.0 GeV.²⁶ It is apparent that the (p, 2p) cross sections have a pronounced rise similar to the rise in pp cross section, although the rise in (p, 2p) cross section is not as steep and begins at lower energies.

An attempt to reproduce the experimental (p, 2p) excitation function was made using the prescription of Hower and Kaufman for the Ar⁴⁰(π⁻, π⁻n)Cl³⁶ reaction.⁶ These authors were able to fit their cross-section data by taking into account the momentum broadening of the free-particle cross section and the attenuation factor for the outgoing particles. The momentum distribution they used has the form

$$f(p) = p^2 \exp[-p^2/p_0^2], \quad (1)$$

where p_0 is an adjustable parameter. The attenuation factor was taken as $\bar{\sigma}^{-1/2}$, where $\bar{\sigma}$ is the average cross section in nuclear matter for the incident particle. If their method is applied to the present work the cross section for the (p, 2p) reaction should be given by the expression

$$\sigma(p, 2p) = k \langle \sigma(pp) \rangle (1/\bar{\sigma}^{1/2}), \quad (2)$$

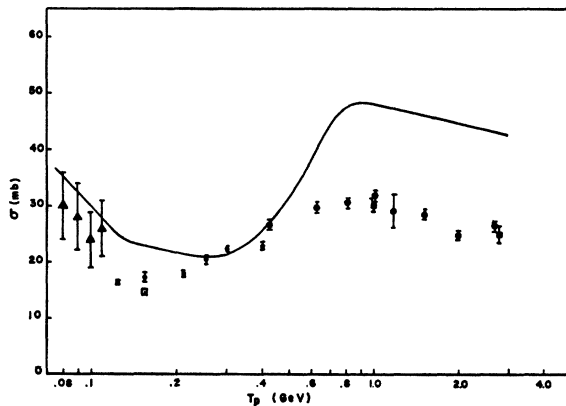


FIG. 4. Excitation function for Mg²⁵(p, 2p)Na²⁴ reaction. Open circles—present work. Closed circles—Ref. 21. Triangles—Ref. 22. Open squares—O¹⁸(p, 2p)N¹⁷ Refs. 23 and 24. Smooth curve—free-particle pp cross section.

²¹ F. M. Kiely, Ph.D. thesis, Carnegie Institute of Technology, 1967 (unpublished).

²² J. W. Meadows and R. B. Holt, Phys. Rev. **83**, 47 (1951). These data have been corrected for revised monitor cross sections and tabulated by A. A. Caretto, Jr., Carnegie Institute of Technology Report No. NYO-10693 (unpublished).

²³ I. Dostrovsky, R. Davis, Jr., A. M. Poskanzer, and P. L. Reeder, Phys. Rev. **139**, B1513 (1965).

²⁴ I. Dostrovsky, H. Gauvin, and M. Lefort, Phys. Rev. **169**, 836 (1968).

²⁵ V. S. Baraschenkov and V. M. Maltsev, Fortschr. Physik **9**, 549 (1961).

²⁶ D. V. Bugg, D. C. Salter, G. H. Stafford, R. F. George, K. F. Riley, and R. J. Tapper, Phys. Rev. **146**, 980 (1966).

where k is a normalization constant and $\langle \sigma(pp) \rangle$ is the effective cross section for pp scattering. $\langle \sigma(pp) \rangle$ was calculated by computer²⁷ from the following expression:

$$\langle \sigma(pp) \rangle = \frac{\iint \sigma(T, p, \theta) f(p) p^2 dp \sin \theta d\theta}{\iint f(p) p^2 dp \sin \theta d\theta}, \quad (3)$$

where $f(p)$ is the momentum distribution of Eq. (1). The parameter p_0 was given selected values from 30 to 800 MeV/c. However, no adjustment of the normalization constant k in Eq. (2) would give a fit to the experimental data for any of the values of p_0 .

An alternative procedure for estimating the excitation function for a simple reaction was used by Poskanzer and Remsburg for the C¹²(π⁻, π⁻n)C¹¹ reaction.⁴ These authors showed that the C¹²(π⁻, π⁻n)C¹¹ cross section could be qualitatively predicted by assuming that the ratio of $\sigma(\pi^-, \pi^-n)/\sigma(p, pn)$ was equal to the ratio of free-particle cross section $\sigma(\pi^-n)/\sigma(pn)$. The assumption was that nuclear structure effects cancelled when the target and product nuclei were the same for two different reactions. The agreement between the predicted and experimental excitation functions improved when they took into account the differences in attenuation factors for incident pions and protons. Kaufman and Hower have analyzed their data on the C¹²(π⁻, π⁻n)C¹¹ and F¹⁹(π⁻, π⁻n)F¹⁸ in the same manner and showed trends in the ratio of π⁻ and p attenuation factors as a function of energy.⁵

We now wish to examine whether the same approach can be used for predicting excitation functions for (p, 2p) and (p, pn) reactions. Even if the target nucleus is the same, the final nuclei are different for the (p, 2p) and (p, pn) reactions which means nuclear structure effects may not cancel. However, Meloni and Cumming have observed that for a Ce¹⁴² target, the two cross-section ratios $\sigma(p, pn)/\sigma(pn)$ and $\sigma(p, 2p)/\sigma(pp)$ have the same shape as a function of incident proton energy in the GeV region.¹⁰ Furthermore, they found that the ratio $\sigma(p, pn)/\sigma(p, 2p)$ was equal to a constant times the ratio $\sigma(pn)/\sigma(pp)$ for the energy region from 0.4 to 28 GeV. In Ref. 11 it was noted that the $\sigma(p, 2p)/\sigma(pp)$ ratio for Zn⁶⁸ and Fe⁵⁷ targets had the same shape as a function of energy as the $\sigma(p, pn)/\sigma(pn)$ ratio for C¹². It therefore seems possible to use the ratio of the cross section for a given simple reaction to the cross section of the corresponding free-particle cross section as an approximation for the relative attenuation factors for some other simple reaction. In particular, we wish to use the $\sigma(p, pn)/\sigma(pn)$ ratio for C¹² to calculate the cross section for the Mg²⁵(p, 2p)Na²⁴ reaction. The C¹²(p, pn)C¹¹ reaction

²⁷ The computer program was a simple modification of the one used in Ref. 6.

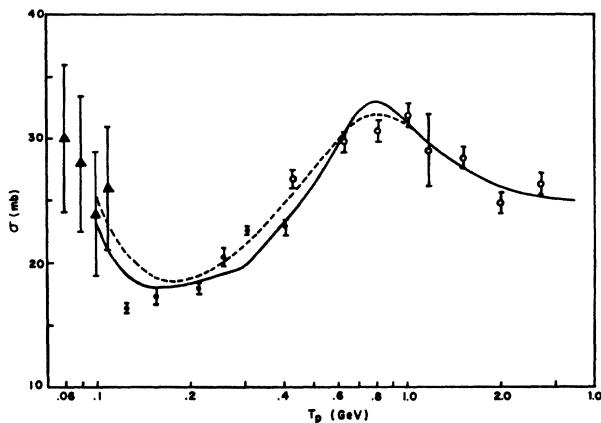


FIG. 5. Calculated $\text{Mg}^{26}(p, 2p)\text{Na}^{24}$ excitation function. Smooth curve—Eq. (4) with free-particle pp cross sections. Dashed curve—Eq. (4) with $p_0=100$ MeV/c. Experimental data: open circles—present work. Closed circles—Ref. 21. Triangles—Ref. 22.

was chosen for this comparison since its excitation function has been carefully studied in this energy region¹² and the target mass is reasonably close to the target mass of interest.

We assume that the cross section for the $\text{Mg}^{26}(p, 2p)\text{Na}^{24}$ reaction is given by

$$\sigma(p, 2p) = k \langle \sigma(pp) \rangle \sigma(p, pn) / \langle \sigma(pn) \rangle, \quad (4)$$

where k is a normalization constant, $\langle \sigma(pp) \rangle$ is the free-particle pp cross section averaged over the momentum distribution of the struck proton, $\sigma(p, pn)$ is the cross section for the $\text{C}^{12}(p, pn)\text{C}^{11}$ reaction at the same incident proton energy as for the $(p, 2p)$ reaction, and $\langle \sigma(pn) \rangle$ is the effective pn cross section calculated in the same manner as $\langle \sigma(pp) \rangle$ with p_0 set equal to 100 MeV/c. This value for p_0 corresponds to the value for p -state protons obtained by Garron *et al.* in an experiment on $(p, 2p)$ scattering from C^{12} .²⁸ $\langle \sigma(pn) \rangle$ differs from $\sigma(pn)$ by less than 3% in the energy range of interest here due to the slow variation of $\sigma(pn)$ with energy. The ratio $\sigma(p, pn) / \langle \sigma(pn) \rangle$ is a crude but simple approximation to the true attenuation factors for the incident and outgoing particles.

Above 1.2 GeV, the effective pp cross sections are equal to the free-particle cross sections for values of p_0 up to 150 MeV/c. Therefore, the normalization constant k in Eq. (4) was determined by averaging values of k calculated for the four highest energy points in Table I. Excitation functions with p_0 values of 50, 100, and 150 MeV/c were calculated from Eq. (4) using $k=0.925$. The excitation function with $p_0=100$ MeV/c gave the best fit to the experimental data above 0.15 GeV and is plotted in Fig. 5 along with the excitation function calculated without taking into account the

momentum distribution. Below 0.15 GeV the $p, 2p$ and p, pn reactions have significant contributions from reaction mechanisms other than the clean knockout mechanism (see below) so Eq. (4) may not be valid at low energies. The value of p_0 obtained here is consistent with p_0 parameters calculated from $(p, 2p)$ coincidence experiments for other light nuclei for the same form of momentum distribution.^{23,29} It should be noted, however, that the momentum broadening is a smaller effect than the variation of the attenuation factors as a function of energy. Hence an accurate calculation of the attenuation factors is essential before trying to use this method to determine momentum distributions.

MONTE CARLO CALCULATIONS

In principle, the cross sections for the $(p, 2p)$ reaction could be calculated using the Monte Carlo method. An accurate treatment by this method for incident proton energies above the meson production threshold is not available. The VEGAS program³⁰ works well for incident proton energies below the meson threshold and was used to calculate the $\text{Mg}^{26}(p, 2p)\text{Na}^{24}$ and $\text{O}^{18}(p, 2p)\text{N}^{17}$ cross sections at an energy of 155 MeV. These two cross sections were first calculated in Israel³¹ using the programs GRACE and EVA. GRACE is a copy of the VEGAS program and EVA is a current version of an evaporation calculation originally created by Dostrovsky, Fraenkel, and Friedlander.³² More extensive results of these calculations have been reported recently.²⁴ The results quoted here were obtained with the normal cutoff parameters in the cascade calculation and a level density parameter a equal to $A/20$ for the evaporation calculation. Calculations were performed with two alternative assumptions—one which assumed no refraction at nuclear potential surfaces and the other which did allow refraction.

Additional calculations were performed using the VEGAS program at Brookhaven National Laboratory.³³ The calculations with and without refraction are labelled as STEP and STEPNO. No evaporation calculation was performed, but the $(p, 2p)$ cross section was obtained as follows. The computer output listed the residual nuclei and excitation energy resulting from the cascade calculation. These lists were scanned to find those events which gave the $(p, 2p)$ product with an excitation energy less than the binding energy of any particle ($n, p, \text{ or } \alpha$). These events correspond to the clean-knockout mechanism. The number of such events was then divided by the estimated fraction of clean-knockout events to obtain the total number of

²⁹ M. Riou, *Rev. Mod. Phys.* **37**, 375 (1965).

³⁰ K. Chen, Z. Fraenkel, G. Friedlander, J. R. Grover, J. M. Miller, and Y. Shimamoto, *Phys. Rev.* **166**, 949 (1968).

³¹ Courtesy of Dr. I. Dostrovsky.

³² I. Dostrovsky, Z. Fraenkel, and G. Friedlander, *Phys. Rev.* **116**, 683 (1959).

³³ Courtesy of K. Chen, G. Friedlander, and J. M. Miller.

²⁸ J. P. Garron, J. C. Jacmart, M. Riou, C. Ruhla, J. Teillac, and K. Strauch, *Nucl. Phys.* **37**, 126 (1962).

(*p*, 2*p*) events. For STEPNO this estimate was obtained directly from the GRACE plus EVA calculation for no refraction.

The nonclean-knockout events are assumed to be mainly due to an inelastic scattering followed by evaporation mechanism (ISE).¹ For STEP, the estimate of ISE events was obtained from the numbers of events leading to a target nucleus at an excitation energy above the binding energy of a proton in the target nucleus but below an energy which would allow evaporation of a proton followed by evaporation of a second particle. For O¹⁸, the number of such events was 1.3 times greater from the STEP calculation than from STEPNO, whereas for Mg²⁵, this ratio was 3.6. The number of ISE events estimated for the STEPNO calculation was increased by these factors to obtain the number of ISE events for the STEP calculation.

The (*p*, 2*p*) cross section was obtained from the fraction of all cascades which end up as the (*p*, 2*p*) product times the total reaction cross section. For the STEP nuclear density model used in all the calculations here, the total reaction cross section was calculated using a nuclear radius expression $R = 1.07A^{1/3} + 2.5$ in units of 10⁻¹³ cm.

TABLE III. Cross sections (mb) calculated by Monte Carlo method for (*p*, 2*p*) reactions at 155 MeV.

Target	Model	$\sigma(p, 2p)$	Percent clean knockout
O ¹⁸	GRACENO ^a	12.3±1.0	97*
O ¹⁸	GRACE ^b	8.7±0.5	
O ¹⁸	STEPNO ^c	16.3±2.7	97 ^h
O ¹⁸	STEP ^d	15.1±2.8	88 ^h
O ¹⁸	Experimental	14.5±0.2 ^e	
Mg ²⁵	GRACENO ^a	29.3±2.9	70*
Mg ²⁵	STEPNO ^c	24.9±4.2	70 ^h
Mg ²⁵	STEP ^d	23.7±4.5	59 ^h
Mg ²⁵	Experimental	17.4±0.7 ^f	

^a GRACE program without refraction (5000 cascades), plus EVA evaporation program.

^b GRACE program with refraction (5000 cascades), plus EVA evaporation program.

^c VEGAS program without refraction (2000 cascades).

^d VEGAS program with refraction (2000 cascades).

^e Reference 24.

^f Reference 21.

* Calculated.

^h Estimated.

The calculated cross sections and percent clean knockout are given in Table III. The results for O¹⁸ are generally in better agreement with the experimental cross section than the results for Mg²⁵. However, STEPNO would give good agreement for the Mg²⁵ calculation if one arbitrarily assumed a much smaller contribution of ISE events as in O¹⁸.

For both O¹⁸ and Mg²⁵ targets, STEPNO predicts more clean-knockout events than STEP. However the resulting (*p*, 2*p*) cross sections are similar for STEPNO and STEP since STEPNO predicts fewer ISE events than STEP. This similarity has been noted previously for other, more complex reactions on light mass targets.²⁴ However, for medium and heavy mass targets, STEPNO has been found to be definitely superior to STEP for simple reactions.³⁰

CONCLUSION

The ratio of the Mg²⁵(*p*, 2*p*)Na²⁴ cross section at 1.0 GeV to that at 0.43 GeV is 1.19±0.05. The similar ratio for the Ce¹⁴²(*p*, 2*p*)La¹⁴² cross section is 1.47±0.13 from Ref. 10. The ratio of free-particle *p*-*p* cross sections is 1.8±0.1. It was originally expected that the ratio for Mg²⁵ should be closer than Ce¹⁴² to that for free-particle scattering because Mg²⁵ has a larger surface-to-volume ratio than Ce¹⁴².

If one includes the data of Kiely²¹ at lower energies, the rise in (*p*, 2*p*) cross section is quite pronounced (16.5 mb at 0.125 GeV compared to 31.9 mb at 1.0 GeV). The levelling out of the (*p*, 2*p*) excitation function compared to the free-particle cross-section data can be explained in terms of an effective cross section due to momentum broadening and by attenuation factors for scattering in nuclear matter.

ACKNOWLEDGMENTS

I wish to acknowledge several discussions with Dr. J. B. Cumming and Dr. A. M. Poskanzer which stimulated this work. I am indebted to Dr. Cumming for providing the computer program for calculating range-energy curves and to Dr. S. Kaufman for the computer program for averaging cross sections over momentum. I wish to thank Dr. I. Dostrovsky, Dr. G. Friedlander, Dr. J. M. Miller, and Mrs. K. Chen for running Monte Carlo calculations for this work. Valuable discussions with Dr. A. A. Caretto and Dr. F. M. Kiely are acknowledged. Finally, I wish to thank the operating crews of the Cosmotron for providing good beams during the midnight hours.